AERATED OPEN-CHANNEL FLOW AT LOW VELOCITIES AND SHALLOW DEPTHS

by

D. L. Fread and T. E. Harbaugh

CIVIL ENGINEERING STUDIES
UNIVERSITY OF MISSOURI - ROLLA
ROLLA, MISSOURI

HYDRAULIC SERIES BULLETIN

JUNE 1970

AERATED OPEN-CHANNEL FLOW
AT LOW VELOCITIES AND SHALLOW DEPTHS

by

D.L. Fread

and

T.E. Harbaugh

CIVIL ENGINEERING STUDIES

UNIVERSITY OF MISSOURI - ROLLA

ROLLA, MISSOURI

HYDRAULIC SERIES BULLETIN

JUNE 1970

AERATED OPEN-CHANNEL FLOW

AT LOW VELOCITIES AND SHALLOW DEPTHS

by

D.L. Fread

and

T.E. Harbaugh

ABSTRACT

An experimental study was conducted to determine the significant hydraulic characteristics of open channel flow of water, subjected to air entrainment. Artificial air entrainment was accomplished by injecting compressed air into the flowing water from minute, equally-spaced holes along the bottom of an open-channel flume. Gradually varied flows with width to depth ratios in the range of 3 to 5 were studied. The energy losses associated with the air entrainment were determined by comparing the change in the Manning roughness coefficient for nonaerated and aerated flows. It was shown that aeration can result in a 45 percent increase in the Manning Coefficient. The increase in energy losses due to aeration was attributed to: 1) restriction of flow area and flow disturbances caused by the air jets near the channel bottom, 2) increased secondary flow of a double spiral pattern, 3) increased boundary frictional resistance due to the bubble layer at the water surface, and 4) flow disturbances and eddy losses resulting from the ascension of discrete air bubbles to the surface of the flowing water. (Key words: aerated, open-channel flow, Manning roughness coefficient).

AERATED OPEN-CHANNEL FLOW AT LOW VELOCITIES AND SHALLOW DEPTHS

by D.L. Fread† and T.E. Harbaugh††

INTRODUCTION

At the present time, considerable emphasis is being given to the purification of our rivers, canals, and lakes by increasing the dissolved oxygen content of the water. Various methods are being employed which cause air, in the form of small bubbles, to become entrained in the water for a sufficient time to allow a portion of the oxygen content of the air to be transferred to the water as dissolved oxygen.

Aerated flow may occur naturally in open channels of steep slope having high-velocity flow and an accompanying high degree of turbulence. This type of aerated open-channel flow is defined as self-aerated flow. Considerable research has been directed toward this type of aerated flow since the early 1950's. Notable works in this area include those by Straub and Anderson (1955, 1958).

Aerated flow may also occur in open channels of mild slope having low velocities of flow. However, in this type of aerated flow, the air must be entrapped in the flowing water by means other than the mechanism of a high degree of surface turbulence produced by high-velocity flow. In low-velocity or artificial aerated flow, the air enters the flowing water as the result of energy which originates

---

† Research Assistant in Civil Engineering, University of Missouri-Rolla, Rolla, Missouri

†† Associate Professor of Civil Engineering, University of Missouri-Rolla, Rolla, Missouri

externally from the flowing water, itself. One type of artificial aerated flow may result from a high-velocity water jet discharging into open-channel flow. Here, the air is entrapped in the flow by the surface turbulence generated by the impact force of the jet; also, air is carried into the flow directly by the jet. Einstein and Sibul (1954) have investigated this type of aerated flow. Another type of artificial aerated flow may result when mechanical agitators produce sufficient surface turbulence in open-channel flow to cause air to become entrained at the free surface (Amberg, Pritchard, and Wise, 1966).

A third type of artificial air entrainment occurs when diffused compressed air is injected into open-channel flow. Townsend (1934) reported on a small number of observations concerning the retarding effect of entrained air bubbles on the flow of a mixture of water and activated sludge through a conventional activated sludge sewage treatment unit. Compressed air was introduced into the sewage through porous plates located along the bottom of the activated sludge basin. Townsend assumed that the hydraulic properties of the mixture of water, activated sludge and entrained air bubbles were the same as for water alone. He concluded that: 1) resistance to flow increases because of entrained air bubbles and this resistance (expressed as Manning n) increases as the flow velocity decreases, 2) an increase in the wetted perimeter due to the air bubbles results in a corresponding decrease in the hydraulic radius, 3) an inverse relationship exists between flow retardance and flow velocity due to greater bubble coalescence occurring at higher velocities causing a decrease in the total wetted perimeter of the entrained air bubbles.

This paper is concerned with a further examination of artificial aerated flow in an open channel. The aeration was produced by

introducing low pressure compressed air into the flowing water from minute, equally-spaced holes located along the channel bottom. The discharge of the open-channel flow was controlled by an adjustable sluice gate at the flume outlet which produced varied, subcritical flow with a backwater curve. Varied flow was investigated as it was impossible to attain uniform flow with the existing experimental apparatus. The objectives of the investigation were: (a) to determine the concentration profile of air in the aerated flow, (b) to determine the increase in depth, i.e., "bulking" due to the presence of the entrained air bubbles, (c) to compare velocity profiles of aerated and nonaerated open-channel flow, and (d) to determine the effect of aeration on the energy losses incurred in open-channel flow.

In this investigation of artificial, aerated open-channel flow, the following basic assumptions were made: (a) the hydraulic principles applying to nonaerated open-channel flow were also applicable to aerated flow, (b) the aerated flow was considered to have the same physical properties, e.g., density, viscosity, etc., as nonaerated flow, and (c) the air injected into the flowing water was considered to affect only the kinematic properties of the flowing water, i.e., the injected air acted upon an elemental volume of water in a manner similar to that which would occur if the injected media were water rather than air.

BACKGROUND

FLOW RESISTANCE: The retardance of flow in open channels is usually evaluated in terms of the Manning roughness coefficient (n) which accounts for the energy losses that occur as a result of the frictional resistance encountered at the channel boundary. However, it is well known that energy losses other than those due to boundary

frictional resistance also occur in open-channel flow, i.e., losses due to secondary flow, eddies, etc. hen an n value is determined for a straight, uniform length of channel, these other energy losses, if present, are combined with the boundary frictional resistance. Therefore, in this investigation, the flow retardance due to the injected air was likewise evaluated in terms of the Manning roughness coefficient (n). However, if one objects to this liberty, the n value so determined may be thought of as an apparent n.

FLOW PROFILE: When a sluice gate is installed in an open channel having steady subcritical flow, the flow will back-up behind the gate such that the depth of flow gradually decreases along the reach of channel in an upstream direction from the gate. The resulting flow equations of Manning and Chezy are invalid for this type of flow.

Referring to Figure 1, the total head at the upstream section 1, above the datum plane coinciding with the channel bottom, is:

$$H = z_1 + y_1 + \alpha_1 V_1^2 / 2g \qquad (1)$$

where: H is the total head, in ft.; z is the distance from datum line to channel bottom, in ft.; d is the depth of flow, in ft.; θ is the bottom slope angle; α is the velocity distribution coefficient; V is the mean velocity, in ft/sec; and g is the gravity acceleration constant, 32.2 ft/sec^2. It is apparent that, with a constant flow rate (Q),.the depth (d) and the mean velocity (V) are a function of the distance (x) measured along the channel bottom. The values of θ and α are assumed constant throughout the channel reach under consideration and θ is considered small. Equation (1) may be differentiated with respect to x to obtain:

$$\partial H/\partial x = \partial z/\partial x + \partial y/\partial x + \partial(\alpha V^2/2g)/\partial x \qquad (2)$$

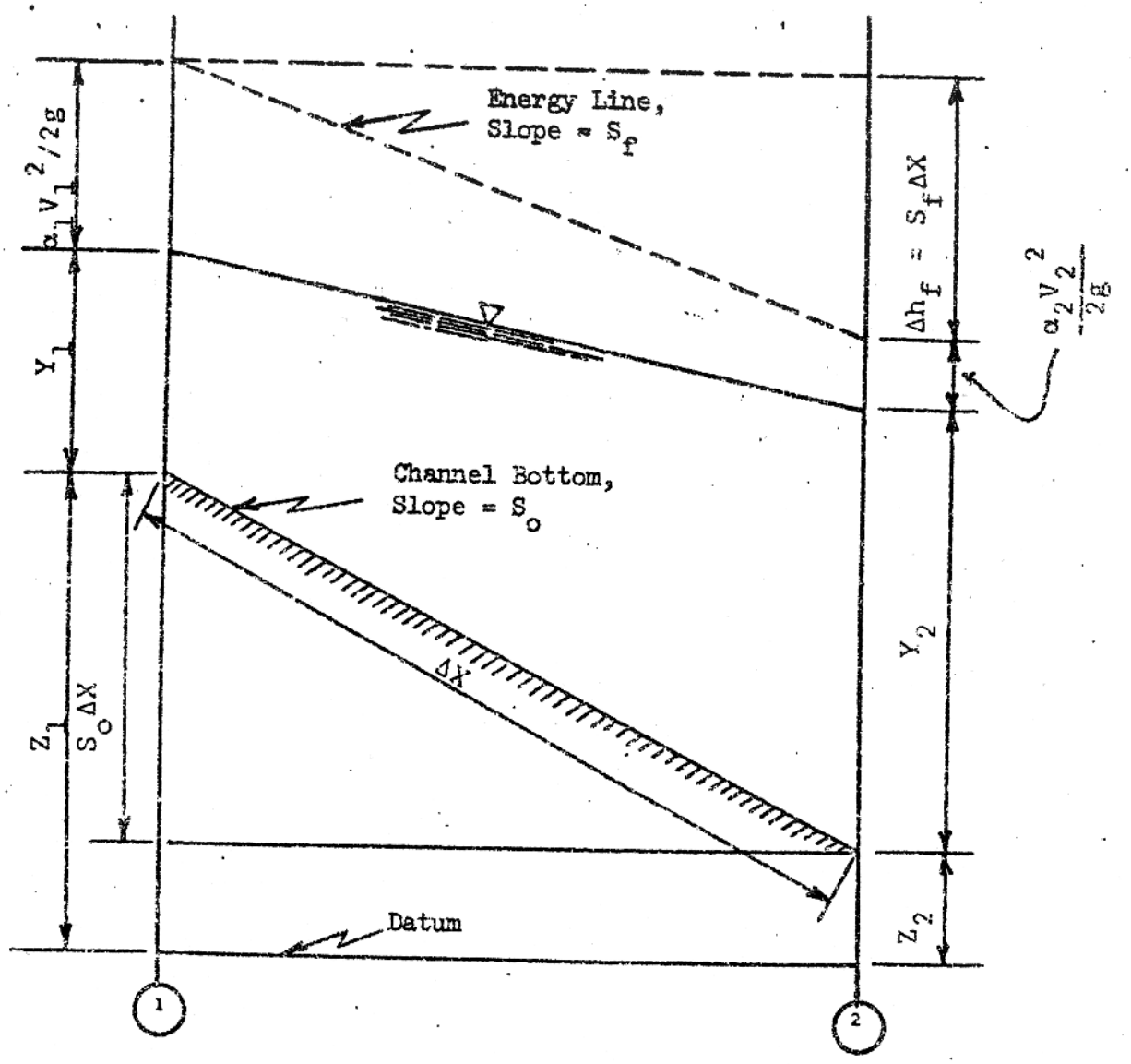

Figure 1. Elemental Reach of Open Channel with Gradually Varied Flow

Since the friction slope (S_f) is equal to $-\partial H/\partial x$, and the slope of the channel bottom (S_o) is equal to $\sin\theta$ or $-\partial z/\partial x$, Equation (2) may be rewritten as the differential equation of gradually varied flow:

$$\partial y/\partial x = (S_o - S_f) / \{ 1 + \partial(\alpha V^2/2g)/\partial y \} \qquad (3)$$

NUMERICAL SOLUTION: Equation (3) may be solved by the direct step method for the flow profile. The distance (Δx) is thus determined for which a given change in the depth (Δy) occurs. In this method, the channel is divided into short reaches of length (Δx), as shown in Figure 1. Assuming the uniform flow equations of Manning or Chezy are valid over the Δx reach of channel, the computation is performed step by step along the channel from a point of known depth to any desired upstream point. The value of Δx corresponding to a relatively small change in y is computed by equating the heads at the two end-sections 1 and 2. Thus,

$$S_o\Delta x + y_1 + \alpha_1 V_1^2/2g = y_2 + \alpha_2 V_2^2/2g + S_f\Delta x \qquad (4)$$

Solving for x yields:

$$\Delta x = (E_2 - E_1) / (S_o - S_f) = \Delta E/(S_o - S_f) \qquad (5)$$

where E is the specific energy at a section and is equal to the sum of the depth (y) and velocity head ($\alpha V^2/2g$) at that section. S_f can be computed from the Manning equation written in the form:

$$S_f = n^2V^2 / (2.22\ R^{4/3}) \qquad (6)$$

where n is the Manning roughness coefficient; R is the hydraulic radius, which is equal to the flow cross-sectional area (A) divided

by the wetted perimeter (P).

The direct step method as explained by Chow (1959) determines the distance along the channel reach at which a specified depth of flow occurs. In this situation, the variables which are known (measured or assumed values) are: the depth of flow (y_1) at an initial point along the channel reach, usually at the point of flow control (in this case the sluice gate); the depth of flow (y_2) which is specified; the steady discharge (Q); the channel geometry, which must be prismatic when using the direct step method; and the Manning roughness coefficient (n). The value of the distance (L) along the channel reach from y_1 to y_2 is then determined by the summation of all the Δx values as computed in the direct step method utilizing Equation (5).

In this investigation, the direct step method was employed in reverse to determine one of the above known values when the distance (L) was known. Thus the Manning n was determined when L, y_2, Q, and the channel geometry were known. A value of n was assumed, and the distance (L) as computed from the direct step method was compared with the actual distance (L) between the points at which y_1 and y_2 occur. If the computed value did not agree with the actual value, n was incremented and the procedure was repeated until the two values of L were the same. The n value at which the two distances agreed was the desired value of n for that particular flow condition. The iterative procedure for determining n was programmed for convenient solution by a digital computer.

EXPERIMENTAL APPARATUS AND PROCEDURE

A plexiglass open-channel flume was the principal apparatus employed in this investigation. The flume measured 36 feet in length,

and 2 feet in both height and width. A plexiglass false-bottom consisting of eighteen separate compartments each 2 feet in both length and width and $2\frac{1}{2}$ inches in height, was placed along the bottom of the flume for the purpose of diffusing compressed air into water flowing in the flume. Compressed air from a centrifugal blower, rated at 300 cubic feet per minute at 15 inches of water pressure, discharged into a 3 inch diameter plastic header pipe. Fourteen $1\frac{1}{2}$ inch diameter valved takeoffs routed the air to the centermost fourteen compartments of the plexiglass false-bottom. The air then passed into the flume interior through minute holes (0.040 inches in diameter) drilled through the 3/8 inch thick plexiglass false-bottom; the holes were equally spaced on one inch centers. U-tube water manometers were provided at each of the fourteen air distribution compartments to monitor the air pressure.

Depth of flow was measured in stilling wells using point gauges graduated to 0.001 ft. Air concentrations were taken with a resistance probe similar to that described by Lamb and Killen (1952). It was powered by an audio frequency oscillator and the measurements were observed on a standard voltmeter.

The flume discharge was controlled and measured by a calibrated sluice gate located at the outlet of the flume. The discharge ( ) was calculated from Equation (7).

$$Q = 5.67\ wbC_d\sqrt{y_1} \qquad (7)$$

where w is the flume width, b is the height of gate opening, y_1 is the depth directly upstream of the sluice gate, and C_d is the discharge coefficient of the sluice gate. C_d was experimentally determined and expressed as a function of the ratio (y_1/b).

Thirteen of the aeration compartments producing 26 ft. of aerated open-channel flow were used throughout the investigation. Velocities were determined with a Price pygmy current meter for representative nonaerated and aerated flows at selected grid points across a flow-section located at the mid-point of the aerated channel. Air concentrations of various aerated flows were determined with the resistance probe and voltmeter at selected grid points across several flow-sections. Depth measurements at the mid-point of the aerated reach of channel were made in the stilling well and in the flume to determine the magnitude of bulking. The depth measured inside the flume corresponded to the average maximum height of the bubble layer which floated on top of the aerated flow. The depth of flow measured in the stilling well essentially corresponded to the depth of an identical nonaerated flow.

Depths for determining the flow retardance were measured in stilling wells located 30.33 ft. apart and at each end of the reach of aerated channel. Discharges ranged from 0.30 to 1.30 cfs for nonaerated and aerated flow. Depending upon the magnitude of the differential pressure between the inside of the air distribution compartments and the static head of the flowing water directly above the compartments, the aerated flow was classified as "maximum air" or "minimum air". The average differential pressure was 2.2 and 1.25 inches of water for maximum air and minimum air, respectively.

RESULTS AND DISCUSSION

AIR CONCENTRATION: The measured air concentration ($\bar{c}$), of the aerated flow represented the average ratio of air volume to water volume flowing between the two electrodes of the resistance probe during a time interval. The air concentrations were determined for

various aerated flows at selected grid points across the flow-section. These were plotted, and "isocons" (contours of equal air concentrations) were determined. Typical isocons are shown in Figure 2. Maximum air concentrations were obtained in the vicinity of the surface in a region previously referred to as the bubble layer. Regions of minimum air concentration in the isocons were noticed to usually coincide with the regions of maximum velocity in corresponding isovels (contours of equal flow velocities).

Average air concentration profiles for various aerated flows of maximum air and minimum air are shown in Figure 3. Also, the air concentration profile for self-aerated flow (Streeter, 1961) is shown for comparison. The maximum and minimum air concentration profiles were observed to be essentially comprised of three regions:

1. An "air-jet" region at the channel bottom, comprising approximately 15% of the total depth of aerated flow for the maximum air and approximately 5% for the minimum air; here, the compressed air entered the flowing water through the 0.040 inch diameter holes in the channel bottom; the jets were somewhat cylindrical in shape with a diameter of about 3/8 inch.

2. A "discrete bubble" region, comprising approximately 70% of the total depth of the aerated flow for maximum air and approximately 80% for minimum air; here individual bubbles, shaped as deformed oblate spheroids of varying size (1/4 to 3/8 inch diameter), moved upward toward the surface of the water at an angle of approximately 45° to 90° with the channel bottom depending on the velocity of the flowing water; the bubbles were formed as each air-jet broke apart due to the resistance of the water to the upward motion of the jet; the air concentration ($\bar{c}$) remained essentially constant throughout this region; and

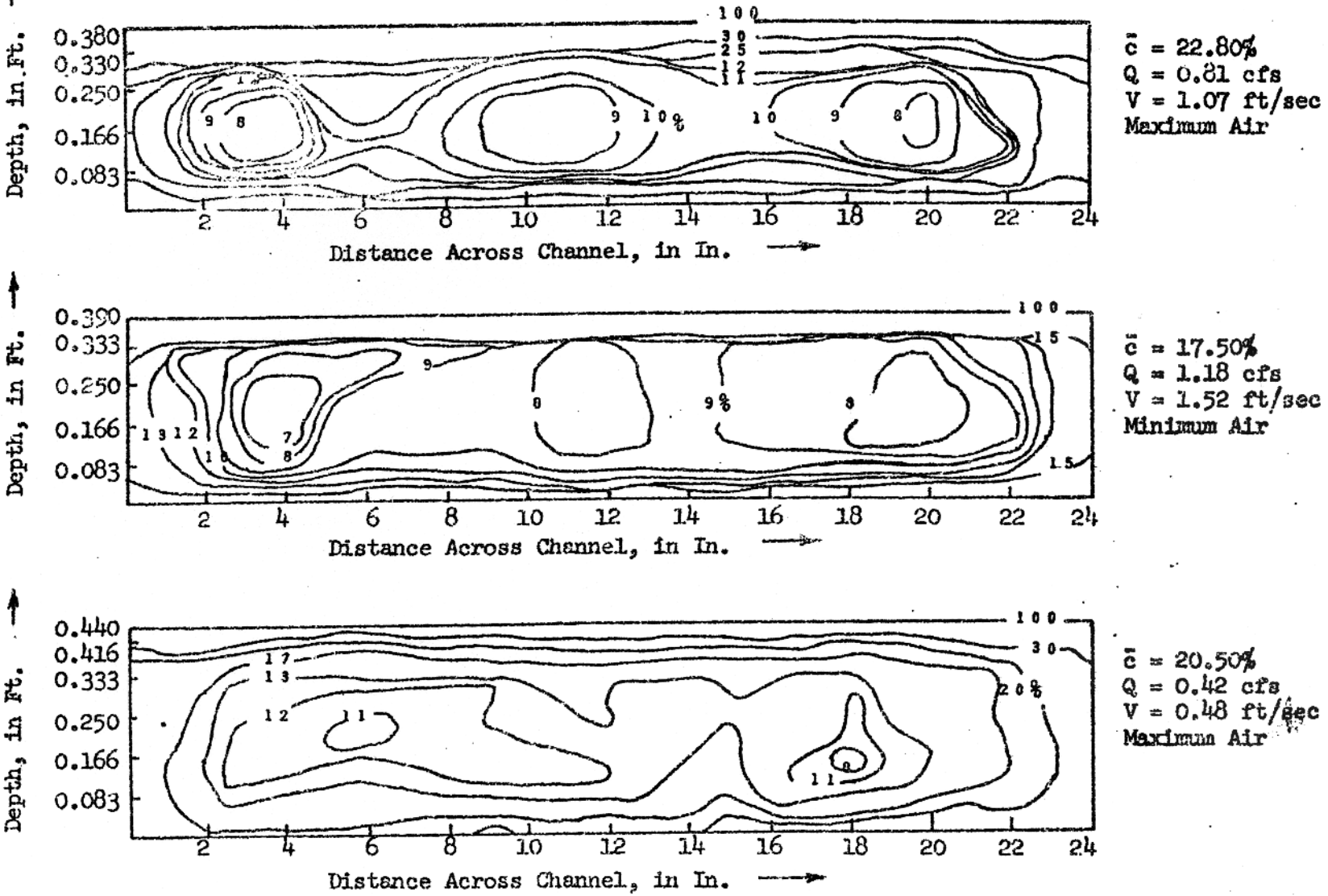

Figure 2. Isocons For Some Representative Aerated Flows

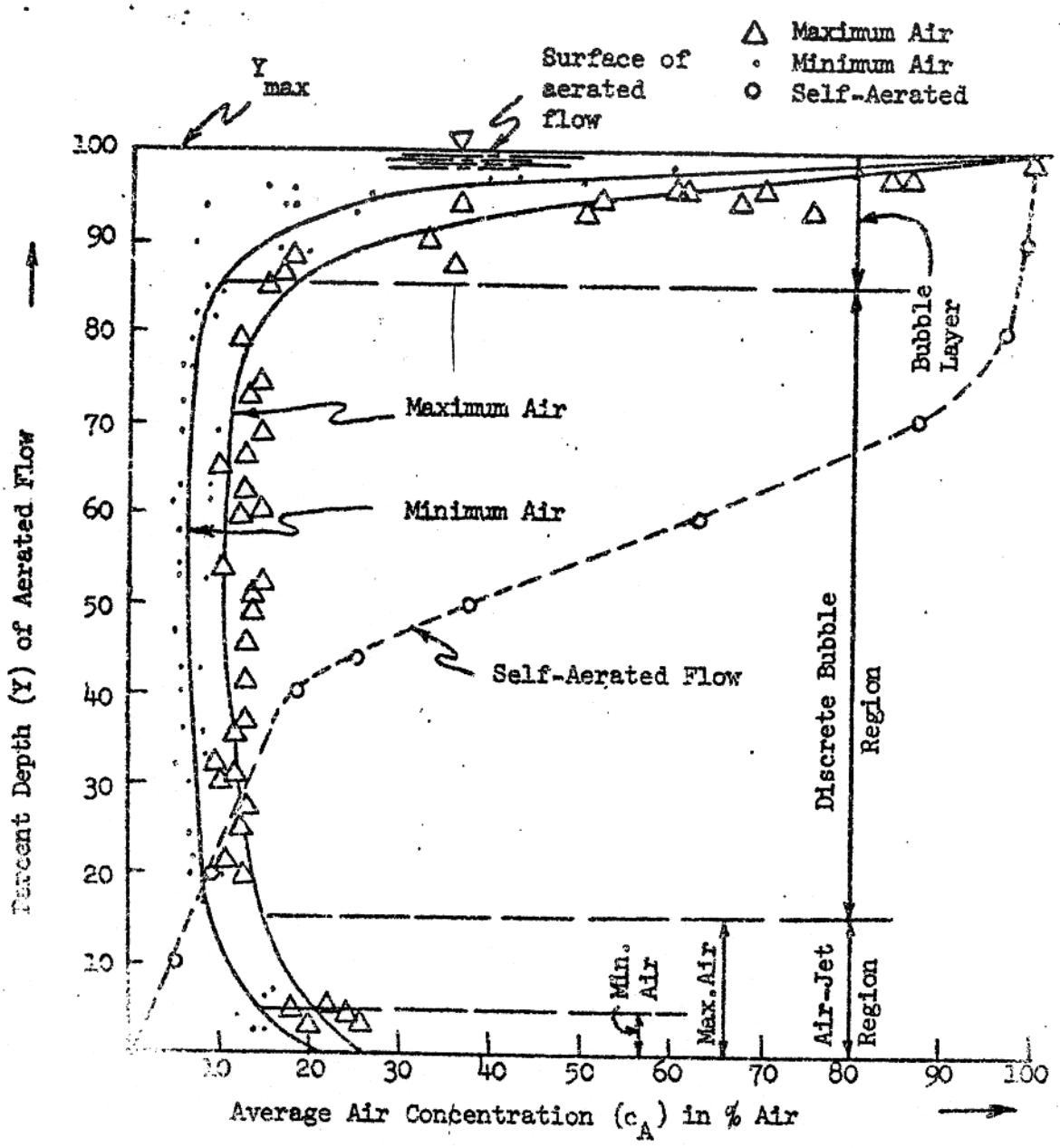

Figure 3. Average Air Concentration (c_A) Profiles of Aerated Flow

3. A bubble layer near the water surface, comprising approximately 15% of the total depth of aerated flow; here, the upward motion of the bubbles from the discrete bubble region was significantly reduced due to the delaying effect of surface tension upon their escape into the overlying atmosphere; this resulted in considerable coalescence of the individual bubbles into larger bubbles; the air concentration ($\bar{c}$) in this region asymptotically approached the value of 100% corresponding to the free surface of the aerated flow.

BULKING: The presence of the entrained air bubbles in the flowing water resulted in an increase in the depth of flow. The ratio of this increase in depth of aerated flow to the depth of a corresponding nonaerated flow was defined as "bulking" (B). Linear correlations of B versus the depth (y) of nonaerated flow are shown in Figure 4 for the two types of aerated flow, maximum air and minimum air respectively. The correlations revealed a significant decrease in B with increasing depth (y) such that the bulking effect appears to approach a level of insignificance as the depth approaches 1.0 foot. However, it is reasoned that this would not be the case if the air input per unit area of channel bottom were increased beyond that corresponding to the maximum air condition of this investigation. Such an increase would result in a correlation curve located parallel to and above those in Figure 4.

VELOCITY: Isovels for representative nonaerated and aerated flows are shown in Figures 5 and 6 respectively. Referring to Figure 6 for the aerated flow, it is apparent there are two regions of maximum velocity located on either side of the flow section generally 2 to 4 inches from the channel sides. In nonaerated flow in rectangular channels of small reach, secondary flow occurs since the flow

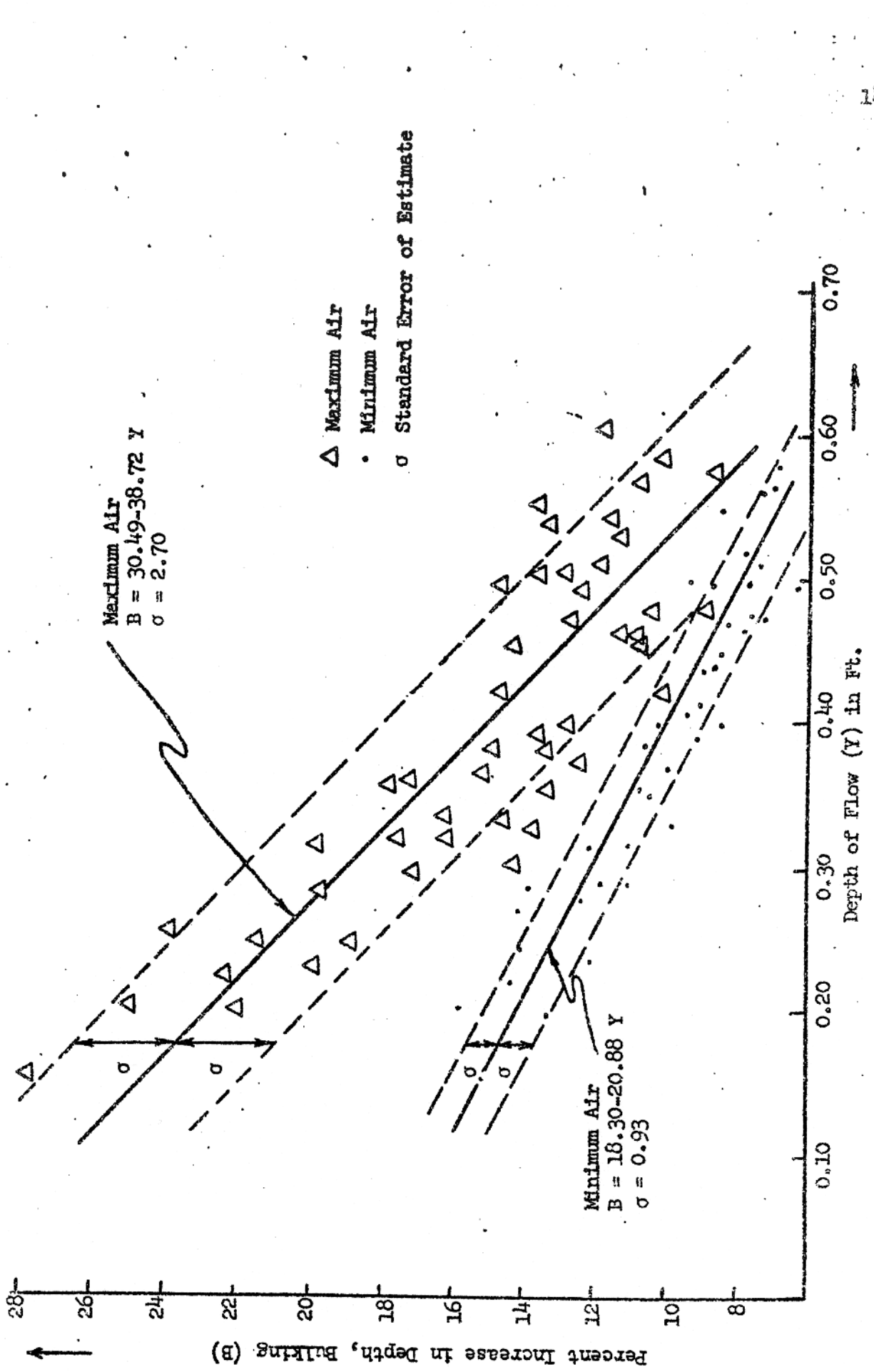

Figure 4. Correlation of Bulking (B) with Depth of Flow (Y)

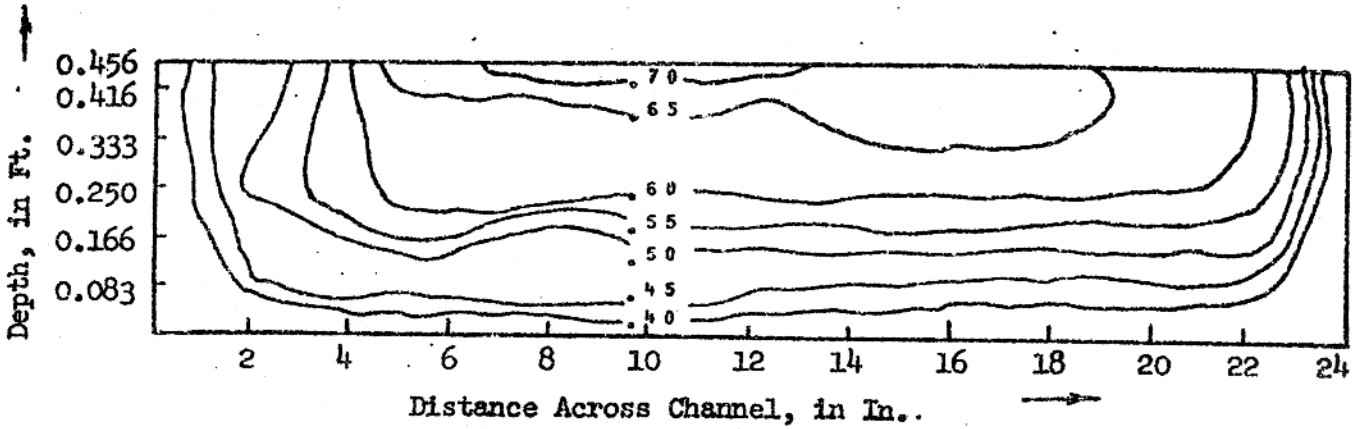

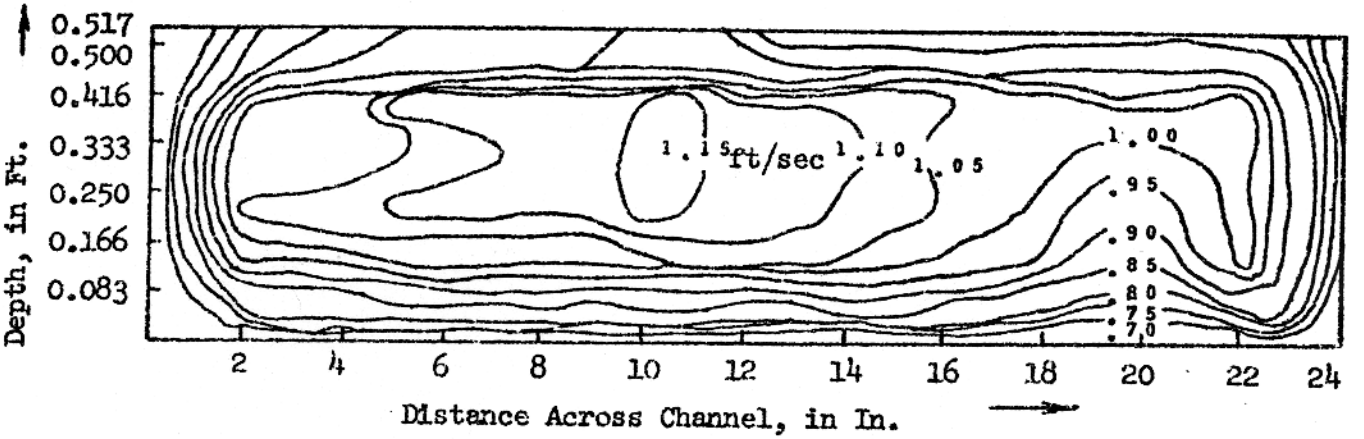

Figure 5. Isovels for Some Representative Nonaerated Flows

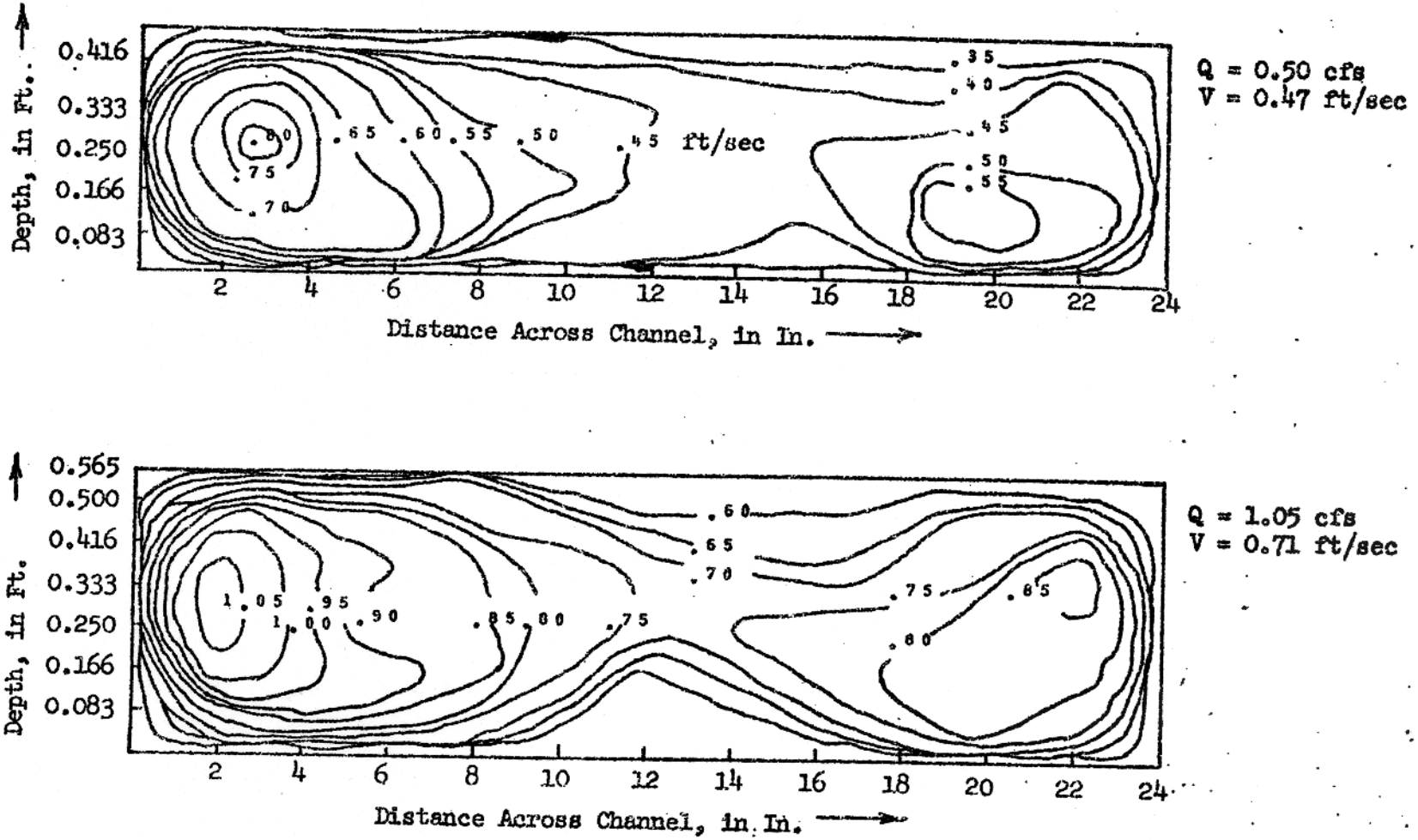

Figure 6. Isovels For Some Representative Aerated Flows

develops along the channel in a single spiral motion (Chow, 1959). In this type of flow, there is one center of maximum velocity as indicated in Figure 5 for nonaerated flow. When the flowing water was subjected to compressed air injected into the flow along the channel bottom, the single spiral motion became a double spiral motion as upward moving air jets cause the single spiral motion to split into two spirals, i.e., the flow consisted of four parallel longitudinal vortices. This occurred at the center of the channel where the spiral flow was essentially horizontal and had no vertical component to resist the upward moving air jets.

The conclusion that a double spiral motion resulted from the injection of compressed air along the channel bottom was further supported by: (a) the surface of the aerated flow, which was comprised largely of air bubbles, was observed to move laterally outwards from the center of the channel towards the channel sides at an angle of approximately 45 degrees, and (b) the air concentrations along the channel sides were greater than the concentrations measured at corresponding depths elsewhere across the flow-section. Thus, at the channel walls, the upward movement of the air bubbles was opposed by the double spiral motion of the flowing water, which moved vertically downward in the vicinity of each channel wall; this caused the air bubbles to remain in the water for a longer period of time, resulting in concentrations of greater magnitude than elsewhere in the flow-section. At all other regions in the flow-section, the flowing water either helped the bubbles to ascend or did not directly oppose their ascension to the surface.

Velocity distribution profiles are shown in Figure 7 for nonaerated and aerated flows. The velocities used therein were arithmetic averages of point velocity measurements taken across the flow section. These were plotted as a ratio (V/V_{max}) of the average velocity (V) at any

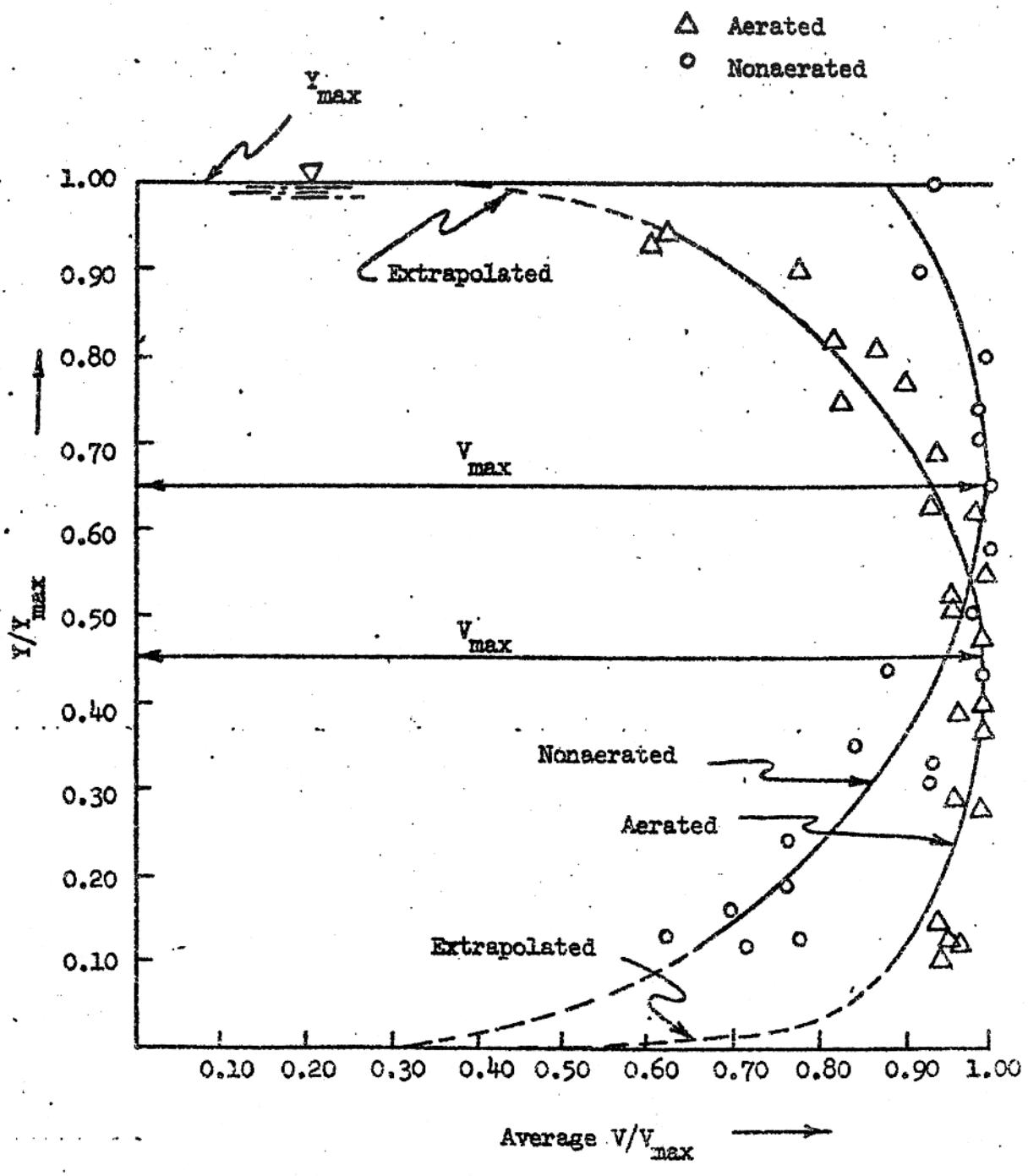

Figure 7. Typical Velocity Profile for Aerated Flow

depth to the simultaneous maximum velocity (V_{max}). The depth of flow was plotted as a ratio (y/y_{max}) where y was the depth of flow at which a particular velocity was measured and y_{max} was the maximum depth of flow associated with that particular velocity and depth measurement. The data points were averages of several flow rates in order to present velocity distribution trends for nonaerated flow as compared to aerated flow.

The velocity distribution profile for the aerated flow differed noticeably from that of the nonaerated flow. Noticeable variations were: (a) the point of maximum velocity of the aerated flow was depressed farther from the surface than in the nonaerated flow; the maximum velocity of the aerated flow was located at 45% of the depth of flow as compared with 65% of depth for the nonaerated flow; and (b) the velocity decreased at a much greater rate as the surface was approached. The surface velocity of nonaerated flow was about 90% of V_{max}; this compared with a velocity of 70% of V_{max} for the aerated flow; this velocity was measured at 90% of the depth of flow in the region just beneath the bubble layer. The variations were attributed to the retarding effect of the bubble layer which comprised approximately 15% of the depth of flow. It was visibly apparent that the bubble layer was traveling at a much lower velocity relative to the adjacent lower region containing discrete air bubbles. Thus, the bubble layer formed a fourth surface causing the open-channel flow to approach that of a closed conduit. This is evident from the similarities between the velocity profile of Figure 7 and that of a pipe flow velocity profile where the velocity asymptotically approaches zero at the pipe wall.

FLOW RETARDANCE: The combined flow retardance due to the frictional resistance at the channel boundaries and that due to the injected air was evaluated in terms of the Manning roughness coefficient (n),

utilizing an iterative solution of the differential equation of varied flow.

Figure 8 shows a correlation of the Manning n with the parameter VR, where V is the mean velocity and R is the mean hydraulic radius for nonaerated flow. The n of the aerated flow (minimum air) is approximately 125% that of the nonaerated flow, and the n of the aerated flow (maximum air) was approximately 145% that of the nonaerated flow. The average value of n for the nonaerated flow was 0.0115 which is within the range of values for channels constructed of material similar to that of plexiglass. The correlation of n with VR is typically used for open channels having a grass lining. The n curve for maximum air is parallel to and approximately 30% of the magnitude of a n curve, given by Chow (1959), for grass-lined channels having a very low vegetal retardance. It appears that there are some aspects of aerated flow due to the injection of compressed air which resembles the flow retardance characteristics of a grass-lined channel. This similarity will be discussed later.

Since, in this investigation, the velocity and depth of flow were the two variables determining the parameter (VR), separate correlations of n with depth and with velocity were also made to provide additional insight into the nature of the increase in n for aerated flow. Correlations of n with the mean velocity (V) along the channel for the two conditions of aerated flow are shown in Figure 9. The n curves for minimum air and maximum air paralleled each other indicating a substantial increase in n with a decrease in the velocity. The tendency toward a decrease in the Manning n with an increase in velocity of aerated flow agreed with the conclusion of Towsend (1934). Correlations of n with the mean depth of flow (y_m) along the channel for nonaerated flow and the two conditions of aerated flow were also made. The n curves for

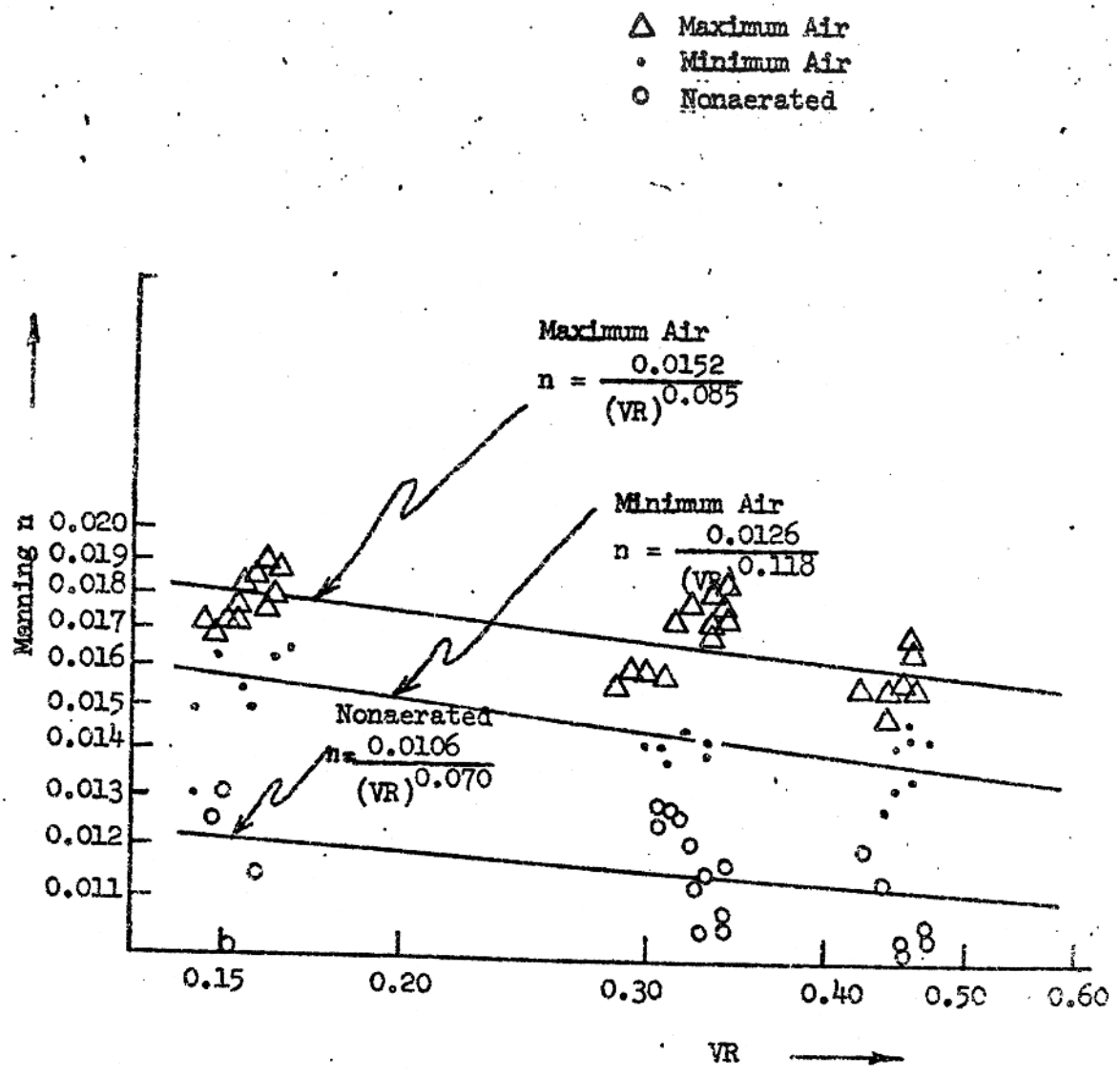

Figure 8. Correlation of Manning n with VR

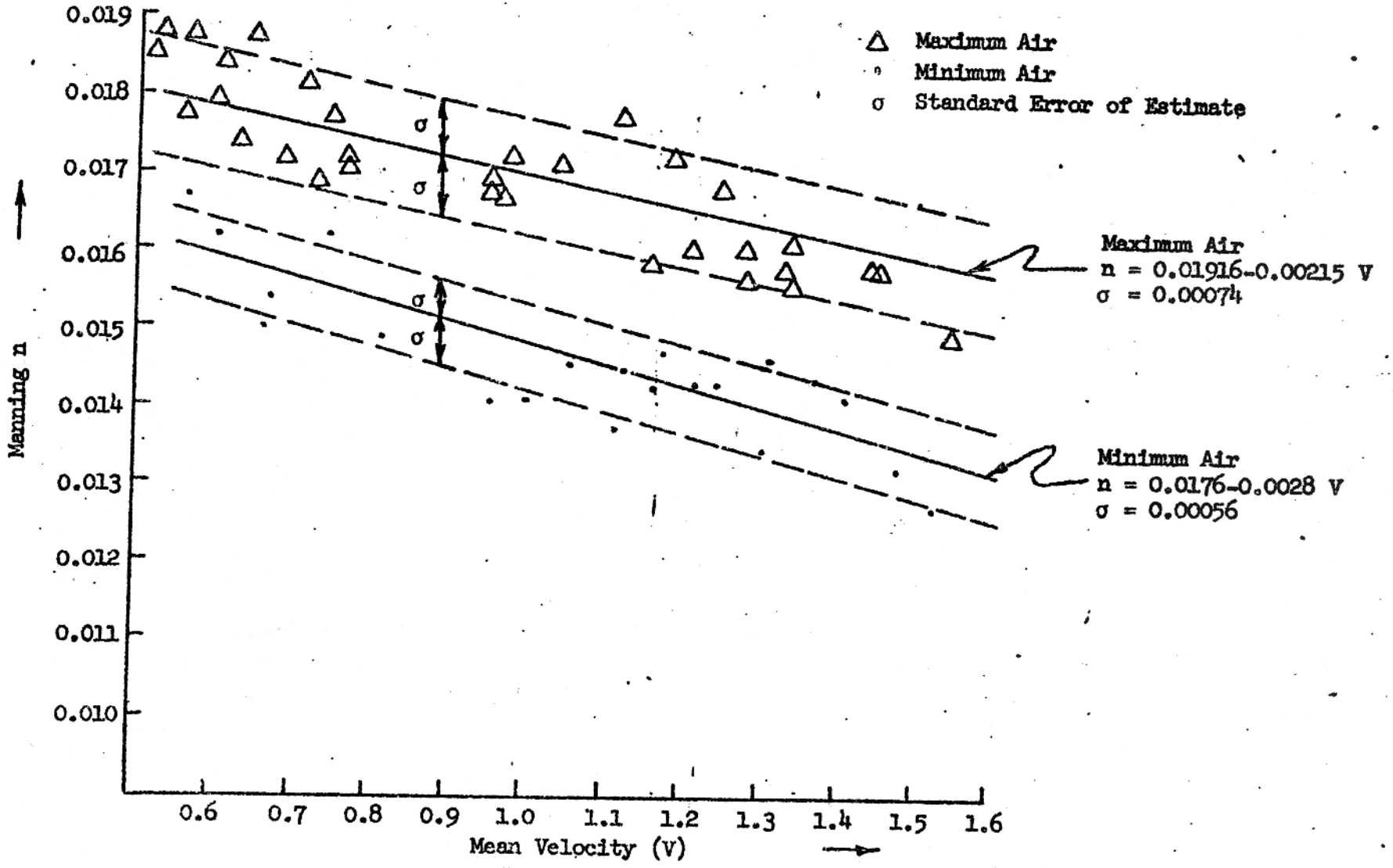

Figure 9. Variation of Manning n with Mean Velocity (V)

nonaerated flow indicated a substantial increase in n with a decrease in depth. This agrees with present hydraulic theory, i.e., as the depth decreases the flow disturbance produced at the channel boundaries influences a greater percentage of the total flow. The n curves for minimum air and maximum air indicated no relationship between n and depth for aerated flow.

In this investigation it was assumed that the Manning roughness coefficient (n) would serve as a means of evaluating not only the degree of flow retardance (energy losses) attributed to frictional resistance at the channel boundary but also those due to other energy losses such as secondary flow, as well as any additional energy losses due to the injection of compressed air along the channel bottom. Thus, for nonaerated flow of this investigation, the factors causing flow retardance were (a) frictional resistance along the channel boundaries (the bottom and the sides), (b) secondary flow due to the single spiral flow prevalent in rectangular-shaped channels, and (c) eddy losses produced in a varied flow of decreasing velocity such as the type of varied flow resulting from a channel restriction, e.g., a sluice gate. Frictional resistance at the channel boundary was the primary cause of flow retardance while secondary flow and eddy losses were minor contributors.

When the same flow was subjected to diffused compressed air injected along the channel bottom, the increase in the energy losses, as noted by an increase in the Manning n, was considered to be due to the following factors: (a) a restriction of the flow area in the air-jet region due to a portion of the flow area being occupied by the air-jets, (b) an energy loss resulting from a disturbed flow due to the air-jets opposing the horizontal movement of the flowing water,

(c) an increase in energy loss due to a greater intensity of secondary flow as evidenced by the double spiral secondary flow induced by the injected air, (d) an increase in the boundary frictional resistance due to the addition of a fourth boundary surface, the bubble layer that floated on top of the flowing water, and (e) eddy losses and flow disturbances produced by the free-floating discrete air bubbles rising through the flowing water.

Referring to factors (a) and (b), the influence of the air-jets on the flowing water somewhat resembles that due to a grass lining of an open channel, (Kouwen, Unny, Hill, 1969). In each case, the flow area is restricted and the flow is disturbed by the projection of the air-jet or blade of grass into the flowing water. As the flow velocity increases, the air-jet or blades of grass, as the case may be, are bent in the direction of the flowing water, and the ratio of restricted flow area to total flow area is decreased. This would seem to account, at least in part, for the decrease in the Manning n with an increase in velocity as was noted in Figure 9.

Referring to factor (e), it is apparent that flow disturbances are produced as the discrete air bubbles travel upward toward the surface through the flowing water. Also, due to viscosity, a wake containing eddies is created as each bubble travels upward. Thus energy losses would arise out of the flow distrubance and eddies created by the ascending bubbles. Noting Figure 8, it is reasonable to assume that as the available air pressure increases above that which was used in this investigation to produce maximum air, the n curve would be located above and parallel to those in Figure 8. This would be due to the air-jets, whose extent of projection into the flowing water is dependent upon the magnitude of the pressure differential

existing between that inside the air diffusion compartments and the static pressure due to the depth of flowing water in the channel. Thus, the greater the available air pressure, the greater would be the retarding effect of the air-jets upon the open-channel flow.

It is interesting to view the results of this investigation from the position that the injected air does have effects upon the physical properties or the flowing water. This is contrary to the basic assumption 2) as stated in the Introduction. From this viewpoint, the injected air would tend to decrease the density and the viscosity of the flowing water. The density would decrease since the air is considerably less dense than the water and since the air does constitute a significant portion of the total volume of the flowing media, a mixture of water and air bubbles. The viscosity would decrease since the air bubbles would act as a lubricant within the flowing media. Such a decrease in density and viscosity would also cause a decrease in the flow retardance as measured by the madnitude of the Manning n. However, since the results indicated a significant increase in the Manning n when the flow was subjected to aeration, this would indicate that the effect of the injected air upon the physical properties is of considerably less magnitude than the effect of the injected air upon the kinematic properties of the flowing water (assumption 3) as stated in the Introduction. This is considered to be due to the extreme importance of the effects of the air jets upon the flow when it is of shallow depth and low velocity.

It would be expected that at greater depths than those of this investigation, the relative importance of factors (a) and (b) would diminish while the importance of remaining factors (c), (d), and (e) would remain essentially constant. Also, the relative importance of the effect of the entrained air upon the physical properties of the flowing media would increase. It is therefore anticipated that some

decrease in the Manning roughness coefficient (n) due to aeration would be expected at considerably greater depths of flow than observed in this investigation.

CONCLUSIONS

Several conclusions were formulated from this investigation of artificial aerated flow. However, they should be restricted to the range of depths, velocities, air pressures and geometry of air diffusion encountered in this investigation.

Aerated flow consists of three regions: (a) an air-jet region located near the channel bottom, (b) a bubble layer located at the free surface, and (c) a discrete bubble region located between the other two regions. The air concentration is essentially constant throughout the discrete bubble region and asymptotically approaches 100% at the free surface of the bubble layer. Bulking will vary directly with air content and inversely with depth.

Air injection induces secondary channel flow of a double spiral pattern. The flow cross-section has two centers of maximum velocity as compared to one for nonaerated flow. The bubble layer at the free surface or the aerated flow produces a frictional resistance which retards the velocity of flow in this region and causes the maximum velocity to occur nearer the mid-point depth than for nonaerated flow.

Aeration produces a substantial increase in the energy losses of open-channel flow. If these losses are considered as flow retardance and expressed in terms of the Manning roughness coefficient (n), they vary directly with the injection pressure of the compressed air and inversely with flow velocity. A 25% and 45% increase in n was noted for the conditions of minimum and maximum air, respectively. Such

increases in the energy losses result from: (a) the air jets at the channel bottom, (b) increased secondary flow, (c) increased boundary frictional resistance due to the bubble layer at the free surface, and (d) flow disturbances and eddy losses resulting from the ascension of discrete air bubbles to the free surface.

REFERENCES

1. Amberg, H. R., Pritchard, J. H., and Rise, P. W., "Supplemental Aeration of Oxidation Ponds with Surface Aeration," TAPPI, Vol. 47, p. 27A, 1964.

2. Chow, V. T., "Open-Channel Hydraulics," McGraw-Hill, New York, 1959.

3. Einstein, H. A. and Sibul, O., "Open Channel Flow of Water-Air Mixtures," Transactions, American Geophysical Union, Vol. 35, No. 2, p. 235, April 1959.

4. Kouwen, N., Unny, T. E. and Hill, H. M., "Flow Retardence in Vegetated Channels," Proceedings, ASCE (Journal of Irrigation and Drainage Division), Vol. 95, No. IR2, June 1969.

5. Lamb, O. P. and Killen, J. M., "An Electrical Method for Measuring Air Concentration in Flowing Air-Water Mixtures," University of Minnesota, St. Anthony Falls Hydraulic Laboratory Technical Paper No. 10, Series B, March 1952.

6. Straub, L. G. and Anderson, A. G., "The Distribution of Air in Self-Aerated Flow in Smooth Open-Channels," SAF Hydraulic Laboratory Project No. 48, July 1955.

7. Straub, L. G. and Anderson, A. G., "Experiments in Self-Aerated Flow in Open-Channels," Proceedings, ASCE, Vol. 84, No. HY7, December 1958.

8. Streeter, V. L., "Handbook of Fluid Dynamics," Open-Channel Flow by V. T. Chow, pp. 24 - 57, McGraw-Hill, New York, 1961.

9. Townsend, D. F., "Loss of Head in Activated Sludge Aeration Channels," Proceedings, ASCE, Vol. 60, January 1934.